View metadata, citation and similar papers at core.ac.uk

brought to you by CORE

provided by NASA Technical Reports Server

(NASA-CR-163812) COMBUSTION AT REDUCED GRAVITATIONAL CONDITIONS (State Univ. of New York at Stony Brook.) 41 p HC A03/MF A01 CSCL 21B

N81-13104

Unclas
G3/25 29386

COMBUSTION AT REDUCED GRAVITATIONAL CONDITIONS

by

A. L. Berlad, L. S. Wang, N. Joshi,

and

C. I. Pai

State University of New York at Stony Brook

Stony Brook, New York 11794

DEC 1980
RECEIVED
NASA STI FACILITY
ACCESS DEPT.

Prepared for
Lewis Research Center
NASA
Under Grant NSG-3051

TABLE OF CONTENTS

I. INTRODUCTION AND BACKGROUND

Previous studies [1-5] have identified

(1) A range of central scientific questions concerning combustible systems--which are best studied with the aid of a Space Shuttle laboratory facility.

(2) "Flame propagation and extinction in clouds of porous particulates" as one of a select group of important combustion experiments for such Space Lab investigations.

(3) An experimental approach, apparatus, and procedures for the study of item (2), above

(4) A theoretical approach to the necessary understanding of the proposed experiments of item (2), above.

The current research effort is designed to advance the theoretical structures needed for the predictive analyses and interpretations for "flame propagation and extinction for clouds of porous particulates." An effort has also been made to further advance related combustion theory of significance to reduced gravitational studies of combustible media.

Theoretical studies [4-6] of flame propagation through clouds of porous particulates are generally couched in terms of sets of conservation equations and appropriate boundary conditions. Central to the requirement that a flame propagation theory also be useful for flame extinction analyses, is the requirement that the boundary conditions be nonadiabatic. Nonadiabatic boundaries are required for both autoignition theory and for extinction theory. Processes that have been considered include, among others, pyrolysis and vaporization of particulates, heterogeneous and homogeneous chemical kinetics, molecular transport of heat and mass, radiative coupling of the medium to its environment,

and radiative coupling among particles and volume elements of the combustible medium.

In general, the needed theoretical structures provided thereby should be capable of quantitatively representing:

(a) Steady state flame propagation
(b) Flame extinction limits
(c) Small particle flame behavior and limits
(d) Large particle flame behavior and limits
(e) Effects of apparatus scale
(f) Effects of system transport properties
(g) Effects of variations in kinetic characteristics of combustibles
(h) Autoignition conditions.

It is expected that the results of this investigation will help to provide an analytical model that can be used to

(a) Aid in experiment selection and design
(b) Understand in-space experimental results
(c) Provide a predictive approach to further understanding of combustion for $g \geq 0$.

In addition to the above cited studies, we have performed related theoretical examinations of selected areas in the field of combustion where reduced gravity studies appear promising and where investigations to date appear inadequate. These latter analyses attempt to identify the critical aspects of the associated combustion processes that appear to require investigation under zero-(g) conditions. It is anticipated that these *ab initio* theoretical studies will be useful to our understanding of fundamental phenomena associated with oscillatory combustion.[7,8]

II. GENERAL THEORETICAL CONSIDERATIONS

For a cloud of particles at reduced gravitational conditions, we consider a flame to be propagating in the negative x-direction. The one-dimensionalized, nonadiabatic energy conservation equation can be written for the gas phase components of the system

$$(1) \quad \frac{d}{dx}\left[G(c_g T_g + h_v\right] = \lambda \frac{d^2 T_g}{dx^2} + \frac{dq_R}{dx} + \dot{q}''' + (S_p \dot{q}_p'' N) - \Sigma L_i$$

where

x - axial direction

c_g - specific heat of the gaseous medium

G - mass flow rate

h_v - heat of vaporization of the condensed phase

T_g - Gas temperature

λ - molecular conductivity

(dq_R/dx) - axial component of the divergence of the radiative flux density

$\dot{q}'''$ - heat release rate associated with gas phase chemical reactions

$\dot{q}_p''$ - local rate of a particle's rate of heat release (or heat absorption)

n_p - local concentration of particles

ΣL_i - Sum of the radial heat loss rates due to all transport processes.

Equation (1) provides for either/both exothermic/endothermic processes within a particle's spatial regime, as well as for gas phase chemical kinetics.

The two-dimensionality and further complexities of the radiative-conductive coupling which may be important have been taken to be separable. This latter simplification may not always be useful and an extensive examination of this issue is provided in a later section of this report.

Gasification due to individual particles may be accounted for by the expression

$$\dot{m}_p = A_s \exp(-E_v/RT_p) \tag{2}$$

Within a propagating flame's structure, the total gaseous mass flow rate, G, is not constant, but increases due to the net effect of all gasification processes. Accordingly,

$$\frac{dG}{dx} = A_s \exp(-E_v/RT_p) n_p \tag{3}$$

provides the matching condition which couples the vaporization reaction rate of the particle cloud to the gaseous mass flux increase. The total mass flux rate, G_t, is given by

$$G_t = G + G_p \tag{4}$$

From conservation considerations for the two-phase system

$$-\frac{dG_p}{dx} = +A_s \exp(-E_v/RT_p) n_p = +\frac{dG}{dx} \quad . \tag{5}$$

In previous discussions, we have noted the general approaches to numerical solution of a system of equations such as (1)—(5) subject to appropriate boundary conditions.

Several interesting conditions limit the ranges of parametric conditions within which quasi-steady flame propagation can be achieved. The first of these pertains to an upper limit on the ambient temperature conditions.[9,10] At sufficiently high ambient temperature conditions, autoignition occurs. At or above the autoignition condition, no quasi-steady flame propagation is possible (the system is supercritical). Other parametric conditions which may

limit existence of quasi-steady flame propagation derive from either energy loss to the environment or from inadequate coupling of the two-phase heat and mass transfer mechanisms which are implicit in equations (1)—(5). Both auto-ignition and flame extinction limits are discussed in the following portions of this report.

III. AUTOIGNITION

Ignition and "explosion" supported by a uniform gaseous system has been treated theoretically and reviewed previously.[11] The elements of such a theoretical structure already exist in appropriate nonadiabatic gas phase flame propagation theory. One has only to set all convective flows to zero and examine the classes of solutions for "nonflowing gaseous systems". This has been done.[11] In a similar way, one may reexamine the limiting case for autoignition for a uniform dust cloud of combustible particulates. Data accumulated by the U. S. Bureau of Mines[12] provide a range of empirical "explosibility indices" for clouds of particulates. Autoignition temperatures which are theoretically comparable to those for premixed gaseous systems are derivable from (1)—(5), and related considerations.[13]

The theory of the autoignition of single particles of metal and of coal has received considerable attention.[14-16] However, experiments show that the cooperative effect of the particles in a cloud has a significant influence on the ignition temperature and that the ignition temperature can also be dependent on the system's physical[17,18] parameters. Meese and Skifstad have treated some features of the ignition of clouds of boron particles.[19] Their definition of ignition temperature is rather specific to the type of metal under consideration (boron) and computations are carried out for ignition times. The definitions and the aims, as well as the mathematical treatment developed here, are different and more general. Rumanov and Khaikin developed an approach[20] to ignition of particle clouds. The present work uses methods of the phase-plane[11] to describe ignition conditions resulting from equations (1)—(5), with no convective flows.

We consider the problem of autoignition of a cloud of solid particles uniformly dispersed in a gas with one component of which it can react exothermally. The heat generated by the gas-solid reaction heats the particle and the surrounding gas is heated by particle-gas heat transfer. The mass of gas in the cloud loses heat to the ambient at the cloud boundary (or a vessel boundary as in laboratory experiments[12]). The particles can also directly exchange heat with the ambient through radiation; radiative transfer is included only to indicate its importance in some cases, but is not treated in detail here.

We assume the following:

1) The system is "homogeneous" in the sense of having uniform properties across the cloud. (This is similar to the classical Semenov theory of autoignition in gaseous systems.) We adopt a two-temperature model with one temperature for the particles and another for the gas in the cloud.

2) A heterogeneous reaction occurs at the surface of the particles (for example, if the cloud consists of metal particles in air, this could be a surface oxidation process). We can generalize the assumed surface reaction to the case of vaporizing particles in subsequent analyses. For the case of vaporizing particles, gas phase[11] autoignition conditions similar to those previously discussed are obtainable.

3) The induction period is sufficiently small so that negligible consumption of fuel or oxidant occurs.

4) Heat transfer is represented by Nusselt's number type coefficients. Radiation transfer is negligible.

5) The effects of natural convection are negligible. (These effects can be important for large temperature differences and cloud sizes.)

6) All physical properties are constant.

The "homogeneous" model permits us to write two energy equations for the cloud, one for the particle, and the other for the mass of gas in the cloud. They are

$$M_p C_p \frac{dT_p}{dt} = Q_p - \alpha_1 S_p (T_p - T_g) - L_r \tag{6}$$

and

$$M_g C_g \frac{dT_g}{dt} = N\alpha_1 S_p (T_p - T_g) - \alpha_2 S (T_g - T_\infty). \tag{7}$$

where

M_p - Particle mass

c_p - specific heat of the particulate material

T_∞ - ambient temperature at the boundaries

T_p - temperature of a particle

t - time

Q_p - net rate of heat generation per particle

α_1 - coefficient for heat exchange between particle and gas

α_2 - coefficient for heat exchange between cloud and surroundings

L_r - total rate of heat loss by radiation per particle

N - total number of particles

S - internal surface area of the vessel containing the particulate cloud

S_p - particle-surface area

Y_0 - mass fraction of reacting gas component.

The nature of the above equations suggests a phase-plane representation[11]. The advantage of such a method is that the local stability of a steady state can be inferred from the classification of the corresponding singular point in the phase-plane, even where the defining equations are nonlinear.

In the $T_p - T_g$ phase-plane, the singular points (and the corresponding steady states for the system) are given by solving the following equations simultaneously:

$$N\alpha_1 S_p(T_p - T_g) - \alpha_2 S(T_g - T_\infty) = 0 \tag{8}$$

$$Q_p - \alpha_1 S_p(T_p - T_g) - L_r = 0. \tag{9}$$

Simplifying,

$$Q_p = \frac{\alpha_1 S_p \alpha_2 S}{(N\alpha_1 S_p + \alpha_2 S)}(T_p - T_\infty) + L_r$$

$$= \frac{\alpha_1 S_p}{1 + \frac{N\alpha_1 S_p}{\alpha_2 S}}(T_p - T_\infty) + L_r. \tag{10}$$

If Q_p is an Arrhenius-type rate with an exponential dependence on T_p, the particle temperature, then Eq. (10) would give the familiar Semenov-type distribution of singular points (steady states). The nature (or local stability) of each of these steady states is determined by the first partial derivatives with respect to the phase-plane variables of the expressions on the right-hand side of equations (6) and (7) evaluated at the singular point[11]. For an Arrhenius-like Q_p, it can be shown, by the methods set out in (11) that the two lower singular points would be a node and a saddle point. The critical condition for ignition occurs when the two points merge[11] and is given by

$$\frac{\partial Q_p}{\partial T_p} = \frac{\alpha_1 S_p}{1 + \frac{N\alpha_1 S_p}{\alpha_1 S}} + \frac{\partial L_r}{\partial T_p} \tag{11}$$

The simultaneous solution of Eqs. (10) and (11) (if Q_p is known as a function of T_p) will give the autoignition condition, that is, the value of T_∞ for autoignition. Along with Eq. (9), the following expressions are obtained for T_∞ and T_g:

$$T_\infty = T_p - \frac{(Q_p - L_r)}{\alpha_1 S_p} - \frac{N(Q_p - L_r)}{\alpha_2 S} \tag{12}$$

$$T_g = T_p - (Q_p/\alpha_1 S_p) + (L_r/\alpha_1 S_p). \tag{13}$$

The examination of these equations requires specification of the forms for Q_p and L_r. The effects of radiative loss would be important in high-temperature situations and the expression for L_r should be dependent on the cloud density. However, for the present L_r is set equal to zero.

Some general results can be obtained by examining limiting cases with the help of Eqs. (11)—(13). We assume that Q_p can be described as a simple-surface reaction by:

$$Q_p = S_p A h_c \rho Y_0 \exp(-E/RT_p). \tag{14}$$

Cloud-particle density is proportional to $NS_p^{3/2}/S^{3/2}$ if we assume spherical particle and cloud geometry.

We may now consider several alternate cases:

Case (a): When $N\alpha_1 S_p/\alpha_2 S \quad 1$, Eqs. (11) and (12) reduce to

$$\frac{1}{T_p^2} \exp(-E/RT_p) = \frac{\alpha_2 S}{NS_p} \frac{R}{EA\rho Y_0 h_c} \tag{15}$$

$$= \alpha_2 \left(\frac{S^{3/2}}{NS_p^{3/2}}\right)\left(\frac{S_p^{1/2}}{S^{1/2}}\right)\left(\frac{R}{EA\rho Y_0 h_c}\right)$$

and

$$T_\infty = T_p(1 - RT_p/E). \tag{16}$$

From Eqs. (15) and (16), we can deduce that for the same particle and cloud size, the temperatures at ignition (T_∞ and T_p) decrease with increase in cloud density. For the same density, the ignition temperatures decrease with a decrease in particle size and with an increase of cloud size.

Case (b): When $N\alpha_1 S_p/\alpha_2 S \ll 1$, equations (11) and (12) reduce to:

$$\frac{1}{T_p 2} \exp(-E/RT_p) = \frac{\alpha_1 R}{EA\rho Y_0 h_c} \tag{17}$$

$$T_\infty = T_p(1 - RT_p/E). \tag{18}$$

Equations (17) and (18) represent the single-particle limit in that the cloud parameters are absent from the ignition conditions. The particle-size dependence comes in only through such dependence of α_1, the particle-gas heat transfer coefficient. For stagnant conditions, α_1 is inversely proportional to the particle diameter and the ignition temperatures would decrease as particle size increased. This also suggests that ignition is likely to be observed as occurrences on individual particles rather than as cloud phenomenon.

The limiting-case results above are qualitatively supported by some of the experimental results of Cassel and Liebman[17] on ignition of metal dust clouds. Their Figs. 2 and 3 show that the ignition temperatures fall with increase in dust concentration for a given particle size. The different dependence on particle size in the two limiting cases is also seen by the cross-over of their ignition temperature-cloud density curves for different particle

sizes. The dependence on cloud size seems intuitively to be in the right direction; however, Cassel and Liebman did not investigate this question.

For porous solids, reaction can occur throughout the solid volume and Q_p changes to (assuming spherical particles):

$$Q_p = S_p^{3/2} A h_c \rho Y_0 \exp(-E/RT_p). \tag{19}$$

The limiting cases now give the following results:

Case (a):
$$\frac{1}{T_p^2} \exp(-E/RT_p) = \alpha_2 \left(\frac{S^{3/2}}{N S_p^{3/2}} \right) \frac{1}{S^{1/2}} \left(\frac{R}{EA\rho Y_0 h_c} \right) \tag{20}$$

and

$$T_\infty = T_p(1 - RT_p/E). \tag{21}$$

Case (b):
$$\frac{1}{T_p^2} \exp(-E/RT_p) = \frac{\alpha_1}{S^{1/2}} \frac{R}{EA\rho Y_0 h_c} \tag{22}$$

and

$$T_\infty = T_p(1 - RT_p/E). \tag{23}$$

In Case (a), the ignition temperature at constant cloud density is independent of particle size, while a decrease with increase of particle size is shown for Case (b).

From this brief examination, it appears that the phase-plane technique can be fruitfully employed in determining autoignition conditions for dust clouds. The ignition conditions derived show qualitative agreement with certain experimental measurements on metal-particle clouds. The method can be extended to study systems with different chemistry and including radiative cooling. However, it appears necessary tocarry out autoignition experiments at reduced gravatational

conditions if energy transport is to be restricted to conduction and radiation and if truly homogeneous clouds of particulates are to be studied.

IV. FLAME EXTINCTION

In the study of premixed, gaseous flames it is found that extinction limits for flame propagation are associated with a number of critical conditions beyond which integrated heat release rates (for the flame structure) cannot match the integrated heat loss rates (integrated over all boundaries) sustained by the flame structure.[21-23]

Equations (1)—(5) characterize a gas phase medium which, if it is to support flame propagation through a cloud of porous, vaporizable solids, must be supplied with adequate gaseous fuel for combustion. Accordingly, it is immediately clear that the boundaries of interaction for the gaseous medium (of this two-phase system) are important in ways which don't apply for pure gas phase media. These include:

(1) Heat losses from the gaseous medium to the particulates are required to support the vaporization process which is necessary for provision of gaseous fuel.

(2) The rate of heat loss sustained by the gaseous component (of the two-phase system) includes, as boundary losses, both the apparatus boundaries which enclose the particulate cloud and the sum of energy losses to the vaporizing particulates.

(3) Hot, optically inactive gaseous components of flame gases may indirectly sustain local flame radiation loss rates via the radiative coupling among particulates as well as the radiative interaction between the particulate cloud and the cold boundaries of the reactive medium.

(4) Vaporizable materials for which (E_v) is very high and for which particle sizes are large (at constant total particle mass concentrations) will generally fail to support flame propagation. For such a system

(a) volumetric kinetic vaporization rates are very small, except at the highest temperatures (Eq. (2)).

(b) volumetric heat transfer (and vaporization) rates from gas to particles at the highest temperatures are still very slow, due to the small number of particles and the fact that these rates depend upon $(T_g - T_p)$ values.

(c) For a broad range of "prevaporization temperatures", the particulate cloud sustains radiative losses to the boundaries, yet contributes little gaseous fuel to the gas-phase flame system.

These observations are generally in accordance with the qualitative features observed for flame propagation limits. However, quantitative application of the approach discussed herein requires observation of flame propagation and extinction data obtained under conditions of weightlessness[24]. We have noted previously[24] that flame propagation data obtained at normal gravitational conditions suffer from a number of necessary deficiencies. Additionally, when flame propagation rates are at all comparable with particle settling rates, apparent flame extinction (at normal gravitational conditions) cannot be attributed primarily to the transport and kinetic processes discussed here. Accordingly, the limiting two-phase coal flame propagation conditions reported in reference (6) need not at all correspond to what we may observe under zero gravitational conditions. Preliminary observations with lycopodium powder-air flames (at reduced gravitational conditions) are in conformity with this observation.

The Conductive-Radiative Mechanisms of Dust Flames

1. Introduction

Previous theoretical models for propagating coal-dust flames have considered transport mechanisms based upon radiative heat transfer from the hot flame region to the incoming coal/air mixture.[16,25,26] These theories appear to be applicable only to devolatilized char flames wherein the heat release rates are slow. In general, the rapid volatilization in coal-dust flames leads to the formation of thin flame reaction zones where temperature rises steeply. The existence of such thin flame fronts ($\sim$ 1 cm) suggests "the importance of gas phase diffusional (conduction) processes in such flames".[6] In the early theoretical model of Smoot, Horton, and Williams[6] radiative processes are ignored. More recent studies do not consider the general conductive-radiative problem for the reaction zone.

If the optical thickness of a flame front based on the inverse of the Rosseland mean free path is either very large or very small, the effect of radiative processes on the structure of flame reaction zone is expected to be small. In the case of a very large optical thickness, this result is due to the fact that the radiative flux rate is small. In the case of very small optical thickness, this result is due to the fact that the divergence of the radiative flux rate is small. In transparent gaseous flames the Rosseland mean free path is infinite and the corresponding optical thickness is zero. The effect of radiation on such flame structure is therefore not important. In dust flames, the Rosseland mean free path is neither infinite nor zero. Thus, the roles played by radiative transport in dust flames requires further examination.

2. Optical properties of dust-containing media

Methods of analysis of radiative transfer problems vary greatly from medium to medium, depending upon the different optical properties involved. It is therefore necessary to briefly review the optical properties of a typical dust medium. This will be useful in the study of the conductive-radiative theory of dust flames to be formulated. It will also serve to guide us in selecting the analytical tools needed to formulate the theory.

In previous experimental studies[6], coal particles of sizes between 3 μ to 38 μ were used. Due to its ready availability, we shall use the optical properties of carbon black particles (refractive index, 2.00—1.20 i) as an approximation to those of coal particles.

Calculation of Mie solutions for spherical particles with refractive index, 2.00—1.20 i, was carried out by Fahimian.[27] Let the dimensionless particle size, x, be defined as,

$$x \equiv 2\pi r/\lambda,$$

where r is the radius of the spherical particle and λ is the wavelength of radiation. Let K_t, K_s, K_a be the extinction coefficient, the scattering coefficient, and the absorption coefficient, respectively. The dimensionless form of the (extinction) coefficient is called the (extinction) efficiency, X, which is defined as,

$$X_t = K_t/C_n A$$

$$X_s = K_s/C_n A$$

$$X_a = K_a/C_n A,$$

where C_n is the number density of particles and A is the geometric cross-section area of individual particle. The Mie solution predicts the relation

between the efficiency and the dimensionless size. The results[27] are reproduced in Fig. 1 in the forms of $X_t - x$ and $X_s/X_a - x$ curves.

For dust media of known mass concentration of solid particles, C_m, and the size of particles, the spectral extinction coefficient, $K_t(\lambda)$, and the spectral single-scattering albedo, $\pi_0(\lambda)$, can be readily calculated,

$$K_t(\lambda) = X_t(x) C_n A = X_t(x) \left(\frac{C_m}{\rho}\right) \left(\frac{A}{V}\right)$$

$$\pi_0(\lambda) \equiv \frac{K_s}{K_t} = 1 - \frac{1}{\frac{X_s}{X_a} + 1} ,$$

where ρ is the density of the solid phase and V is the volume of the solid particles. For spherical particles,

$$\frac{A}{V} = \frac{3}{4r} .$$

In the ranges of particle sizes and of wavelengths considered, the value of x is greater than unity and the variation of X_t is moderate. With decreasing particle size, the decrease in X_t is moderate and the increase in the area/volume ratio is more pronounced. Consequently, the extinction coefficient increases with decreasing particle size under constant mass concentration. This property, which is displayed in Table 1 and Fig. 2, may effect the dependence of the burning velocity of dust flames on the mass concentration and the particle size (see Fig. 4). We shall come back to this point later in our discussion.

The other significant (optical) property of dust media with particles is this size range and radiation field (in this wavelength range) derives from the fact that the variation of the extinction coefficient and the single-scattering albedo with wavelength is small. It is therefore possible

to consider the idealization of dust-containing media as gray media. A good estimate of the error involved in such a gray approximation is given by the difference of the Planck mean from the Rosseland mean extinction coefficient, i.e.,

$$\frac{K_{tP}-K_{tR}}{K_{tR}},$$

Such an estimate is shown in Fig. 3 and supports fully the use of the gray approximation.

Thus, the adoption of a mean extinction coefficient is made possible.

3. The conductive-radiative transport mechanism

We now consider the relation between heat transfer processes and reaction zone structure and burning velocity. Differences in particle and gas temperature will be ignored.

The energy balance may be written as

$$\alpha \frac{d^2T}{dx^2} - \frac{1}{\rho_a C} \nabla\cdot(r\pi F) + H - w \frac{dT}{dx} + \frac{Q/C}{\tau(T)} = 0, \tag{24}$$

where α is the thermal diffusivity,

$4\pi F (\equiv 4\pi \int_0^\infty F_\nu d\nu)$ is the radiation flux,

H is the conduction and radiation heat loss,

ρ_a is the density of medium,

w is the burning velocity,

Q is the heat of reaction,

$1/\tau$ is the rate of reaction.

For an adiabatic flame, $H = 0$. One may consider equation (24) the equation for the unknown T since F is a known functional of T. The equation is an integral-differential equation with integration over both frequency and

physical space. Such an equation is difficult to solve. However, once the flame is considered as a gray medium, it becomes possible to remove the need of integration not only over frequency space but also over physical space. The approximation which removes the need for integration over physical space is called the diffusion approximation.

The monochromatic radiation flux, $4\pi F_\nu$, may be expressed approximately in terms of the monochromatic Planck's function, B_ν, and the monochromatic mean intensity, J_ν.

$$F_\nu = -\frac{4-\pi_0}{9(1-\frac{1}{3}\pi_1)}\frac{dJ_\nu}{d\tau_\nu} + \frac{1-\pi_0}{9(1-\frac{1}{3}\pi_1)}\frac{dB_\nu}{d\tau_\nu} \quad , \tag{25}$$

where τ_ν is the optical depth and π_1 is the asymetric factor of the scattering phase function. Equation (25), which was derived by using the exponential kernel substitution method[28], reduces in the limit of radiative equilibrium in gray media to

$$J_\nu = B_\nu$$

In the limit of conservative scattering,

$$\pi_0 = 1 \quad ,$$

and the classical Eddington approximation is obtained

$$F_\nu = -\frac{1}{3(1-\frac{1}{3}\pi_1)}\frac{dJ_\nu}{d\tau_\nu} \quad . \tag{26}$$

It has been shown that in the general case this approximation, equation (25) remains quite accurate while the Eddington approximation, equation (26), fails in the case of

$$\pi_0 \ll 1 \quad \text{and} \quad J_\nu \neq B_\nu \quad .$$

With $K_t(\nu) = K_{tR}(\equiv K)$, equation (25) can be integrated with respect to frequency and becomes

$$F = -\frac{4-\pi_0}{9(1-\frac{1}{3}\pi_1)}\frac{dJ}{d\tau} + \frac{1-\pi_0}{9(1-\frac{1}{3}\pi_1)}\frac{dB}{d\tau}, \tag{27}$$

where $B \equiv \int_0^\infty B_\nu d = \frac{\sigma}{\pi}T^4$ and σ is the Stefan-Boltzmann constant. Radiation flux is then expressed, according to the diffusion approximation in terms of temperature and mean intensity. One needs another differential equation which together with equation (24) describes the temperature distribution and the mean intensity distribution. This equation is the emission-absorption equation.

$$\frac{dF}{d\tau} = (1-\pi_0)(B-J). \tag{28}$$

Eliminating F among equations (24), (27), and (28), we have the governing equation for T and J,

$$\alpha\frac{d^2T}{dx^2} - \frac{4\pi}{\rho_a C}(1-\pi_0)K(B(T)-J) - w\frac{dT}{dx} + \frac{Q/C}{\tau(T)} = 0 \tag{29}$$

$$-\frac{4-\pi_0}{9(1-\frac{1}{3}\pi_1)}\frac{d^2J}{d\tau^2} + \frac{1-\pi_0}{9(1-\frac{1}{3}\pi_1)}\frac{d^2B(T)}{d\tau^2} + (1-\pi_0)J - (1-\pi_0)B(T) = 0. \tag{30}$$

With additional equations to describe $\tau(T)$ and with appropriate boundary conditions, these equations can be integrated to determine the eigenvalue, w.

4. Burning velocity of coal-dust flames

Without obtaining explicit solutions to equations (29) and (30), we may examine them to make a qualitative comparision of a conductive-radiative theoretical model with the pure conductive theoretical model of coal-dust flames.

Experimental flame velocity measurements were reported by Horton and Smoot.[6] "In general, a lean flammability limit is evident around 100-200 mg coal dust per liter of air, while maximum flame velocities of 20–35 cm/sec at 300 to 600 mg/ℓ and rich limits well over 1000 mg/ℓ were also observed. In addition, an increased particle size markedly decreased the lean-side and peak flame velocities while causing the peak to occur in a richer flame. However, on the very rich side, a large size increased the flame velocity ... ." A typical example of experimental results together with their theoretical results is reproduced in Fig. 4 .

Consider the small particles of 10 μ at concentrations greater than 500 mg/ℓ. The optical thickness of the flame front is greater than unity. At 1200 mg/ℓ the front optical thickness is about 3, i.e., a moderately large optical thickness. In the limit of large optical thickness, J - B becomes small, i.e.,

$$J \tilde{=} B$$

and equations (29) and (30) reduce to

$$(31) \qquad \frac{1}{\rho_a C}\left[\frac{d}{dx}\left(k\frac{dT}{dx} + \frac{16\sigma T^3}{3(1-\frac{1}{3}\pi_1)K}\frac{dT}{dx}\right)\right] - w\frac{dT}{dx} + \frac{Q/C}{\tau(T)} = 0 \ .$$

The effective "conductivity" is[29]

$$k + \frac{16\sigma T^3}{3(1-\frac{1}{3}\pi_1)K} \ .$$

The heat flux in a pure conductive model is

$$-k\frac{dT}{dx} \ ,$$

while in a conductive-radiative model the heat flux is

$$-k(1+\frac{1}{N})\frac{dT}{dx},$$

where $\frac{1}{N} \equiv \frac{16\sigma T^3}{3(1-\frac{1}{3}\pi_1)kK}$ is a dimensionless parameter measuring the relative importance of radiation and conduction. Thus, consider the example where

$T = 1200°K$

$k = 0.0782$ w/nK for air

$K(1-\frac{1}{3}\pi_1) = 300\ m^{-1}$ (corresponding to roughly 10 μ particles at 1200 mg/ℓ),

we find

$$\frac{1}{N} = 22.$$

Thus the pure conductive model greatly underestimates the effective "conductivity".

The early theoretical model of Smoot, Horton, and Williams[6] should predict a burning velocity which is much lower than the observed values due to its neglect of radiative processes. Yet the model predicts a burning velocity which is actually higher than the observed value (see Fig. 4). It also predicts a maximum temperature which is higher than the observed value.

For 10 μ particles at concentrations less that 500 mg/ℓ and the larger 33 μ particles at all concentrations studied in the experiments (Fig. 4), the optical thickness of the flame front is moderate or small. To the extent that F is related to the gradient of the mean intensity,

$$F \sim \frac{\Delta J}{\Delta \tau},$$

the maximum F will remain of the same order of magnitude regardless of the

opacity of the flame front. However, their distributions will be different, as shown schematically in Fig. 5. For smaller flame front opacity, the radiation flux remains important while dF/dx becomes smaller within the reaction zone in comparison with $(k)d^2T/dx^2$. One expects, therefore, the still considerable F in the preheat zone to raise the temperature of the dusty medium. Within the reaction zone, the overall exothermic reaction continues to increase the temperature through conduction processes. This leads to high maximum temperature in the reaction zone. One may confirm this conclusion from another line of reasoning. In the preheat zone and the post-reaction zone where conduction and heat release are negligible, equation 1 reduces to,

$$w \frac{dT}{dx} = - \frac{1}{\rho_a C} \frac{d}{dx} (4\pi F) ,$$

or

$$T \propto -F .$$

With the opacity of the reaction zone being moderate or small, F in the preheat zone and the post-reaction zone remains significant (see Fig. 5). Temperatures immediately in front of the reaction zone and behind the reaction zone will be raised by the combined conduction-radiation process.

It is therefore expected that a mere pronounced peak of the maximum temperature develops in dust flame when the opacity of the flame front decreases from large to moderate value. The burning velocity should increase markedly with decreasing concentration of 10 μ particles. This is also indicated by the observed burning velocity showing a marked increase and becoming greater than the theoretical prediction of a pure conductive model. For 33 μ particles, the observed burning velocity remains high throughout and at 1200 mg/ℓ, it is actually higher than that of 10 μ dust. According

to the present view, this is due to the pronounced temperature peak which remains in the case of 33 μ at 1200 mg/ℓ. The temperature wanes in the case of 10 μ particles at 1200 mg/ℓ.

Finally, we note that the cited experimental data for coal dust flames[6] were obtained at normal gravitational conditions. Our experience with (preliminary) studies of lycopodium dust flames suggests that apparent lean limit observations (at g = 1) do not correspond to those to be obtained under gravity-free conditions[24]. Also, settling velocities vary with particle size, suggesting that (g = 0) vs. (g = 1) observations differ more substantially as settling velocities (particle size) increase. It is also to be noted that the added sophistication of this conductive-radiative dust flame model is particularly appropriate for flames subject to no gravitationally induced body forces. This is not the case for the data of reference 6. The theoretical approach discussed here is expected to be directly applicable to data derived during Space Shuttle combustion studies.

VI. OTHER COMBUSTION PHENOMENA AND GRAVITATIONAL EFFECTS: OSCILLATORY COMBUSTION OF CARBON MONOXIDE.

In a previous REVIEW [2] we have noted the need for the study of a range of other combustion phenomena at reduced gravitational conditions. In the following pages, we report on our recent studies in one such area, OSCILLATORY COMBUSTION OF CARBON MONOXIDE. In this case we again find that space-based combustion experimentation is needed to verify and/or assist in the development of existent or needed theory.

Previous studies of the oscillatory combustion of carbon monoxide have lead to the conclusions that wall effects are of great importance.[2,30-36] The physicochemical nature of these wall effects have been the subject of substantial discussion, but the essence of these discussions involves the transport of heat and mass between the gas phase oxidative processes and the reactor walls. In general, it is thought that heterogeneous chemical processes at the reactor walls play a key role in defining the oscillatory combustion of carbon monoxide. Inasmuch as temperature gradients between the axial regimes of such (long, cylindrical) reactors appear to be small, it is believed that heat transfer processes between walls and gas phase are of lesser importance than mass diffusion (and heterogeneous kinetic) effects. Accordingly, the oscillatory oxidation of carbon monoxide has been thought to be a purely kinetic oscillation, as distinct from the well-known thermokinetic oscillations found for the oxidation of hydrocarbons.

The theory of kinetic oscillations given by Yang and Berlad[35,37] involves the following chemical kinetic schematics:

$$CO + O_2 \xrightarrow{k_1} CO_2 + O \qquad (1)$$

$$CO + O + M \xrightarrow{k_2} CO_2^*(CO_2) + M \qquad (2)$$

$$CO_2^* + O \xrightarrow{k_3} CO + O_2$$

$$CO_2^* + M \xrightarrow{k_4} CO_2 + M \quad (4)$$

$$CO + OH \xrightarrow{k_5} CO_2 + H \quad (5)$$

$$H + O_2 \xrightarrow{k_6} OH + O \quad (6)$$

$$O + H_2O \xrightarrow{k_7} 2OH \quad (7)$$

$$H \xrightarrow{k_8} \text{destruction on wall} \quad (8)$$

$$O \xrightarrow{k_9} \text{destruction on wall} \quad (9)$$

$$OH \xrightarrow{k_{10}} \text{destruction on wall} \quad (10)$$

$$H + O_2 + M \xrightarrow{k_{11}} HO_2 + M \quad (11)$$

$$HO_2 + HO_2 \xrightarrow{k_{12}} H_2O_2 + O_2 \quad (12)$$

$$H_2O_2 + M \xrightarrow{k_{13}} 2OH + M \quad (13)$$

$$HO_2 \xrightarrow{k_{14}} \text{destruction on wall} \quad (14)$$

$$H_2O_2 \xrightarrow{k_{15}} \text{destruction on wall} \quad (15)$$

$$H + H_2O_2 \xrightarrow{k_{16}} H_2O + OH \quad (16)$$

$$O + OH \xrightarrow{k_{17}} O_2 + H \quad (17)$$

The roles of kinetic wall saturation effects and other heterogeneous kinetics are implicit in schematics (8), (9), (10), (14), and (15). Unlike the (other) rate constants which describe homogeneous gas phase kinetics, k_8, k_9, k_{10}, k_{14}, and k_{15} can be shown, in general, to be functions of tube geometry, tube diameter, a diffusion coefficient, and the concentration gradients which drives species flux rates between walls and gas phase. Consider, then, the diffusive transport of some species, c_i, from the gas phase reaction volume to an absorbing wall. The diffusion equation, in the absence of natural convective effects, can be written

$$(18) \qquad \frac{dc_i}{dt} = D\frac{d^2c_i}{dx^2} + \dot{c}_i'''$$

where, for convenience, the geometric arrangement is taken to be plane parallel plates of infinite extent. The relation to other geometries will be noted later. If the plane parallel plate wall separation is (d) and the reactor extends over the range $-d/2 \leq x \leq +d/2$ and, for a quasi-steady process, equation (18) can be integrated to yield

$$(19) \qquad c_i = \frac{\dot{c}_i'''}{2D}\left[\left(\frac{d}{2}\right)^2 - x^2\right]$$

The mean concentration for the reactor is given by

$$(20) \qquad \bar{c}_i = \int_{-d/2}^{d/2} c_i dx \Big/ \int_{-d/2}^{d/2} dx$$

Then, assuming that $\dot{c}_i'''$ is spatially uniform and that there are no wall reflections, we obtain a relation between the rate of production of the species of interest and the other parameters of the problem.

$$(21) \qquad \left[\dot{c}_i'''\right]_s = \frac{12D\bar{c}_i}{d^2}$$

Thus, for example, for the case of schematic number (10),

$$OH \xrightarrow{k_{10}} \text{destruction on wall, and}$$

the corresponding sink term for [OH] implies

$$(22) \qquad \left\{\frac{d}{dt}[OH]\right\}_{10} = [OH](k_{10})$$

Comparing (21) with (22) shows that

$$\left[k_{10} \equiv \frac{12D}{d^2}\right]$$

A more general expression for k_{10} may be written in the form

$$k_{10} = \left[\frac{ZD}{d^2}\right]$$

where (Z) is a characteristic geometric parameter having the values

Z = 12, for plane parallel plates of infinite extent, and

Z = 32, for cylinders.

It is significant to note the various assumptions that go into the seemingly straightforward schematics which attempt to describe the heterogeneous processes associated with walls. There is the assumption that natural convection is absent and that a known quasi-steady concentration (clearly nonuniform and unsteady for our case) is operative. Even if one accepts these assumptions, the diffusive regime of heterogeneous kinetics depends upon temperature, pressure, vessel size and vessel geometry. Gray[38] has shown that small nonisothermalities in reactors do lead to natural convective transport between walls and reactor volumes.

Systematic variation of reactor vessel size subject to convection-free heat and mass transport has not been carried out for the case of oscillatory combustion of carbon monoxide. Indeed, if such experiments can be carried out under gravity-free conditions, the time and space variations of the various species important to carbon monoxide oxidation could be easily followed (e.g., in a cylindrical reactor) spectroscopically. The gravity-free case permits

true cylindrical symmetry both in the cylindrically uniform heating of the reactor vessel as well as the radially symmetric transport of heat and mass. Such studies would permit observation of a level of experimental detail (Space and time variation of concentrations and fluxes) which have not heretofore been possible.

VII. LIST OF FIGURES

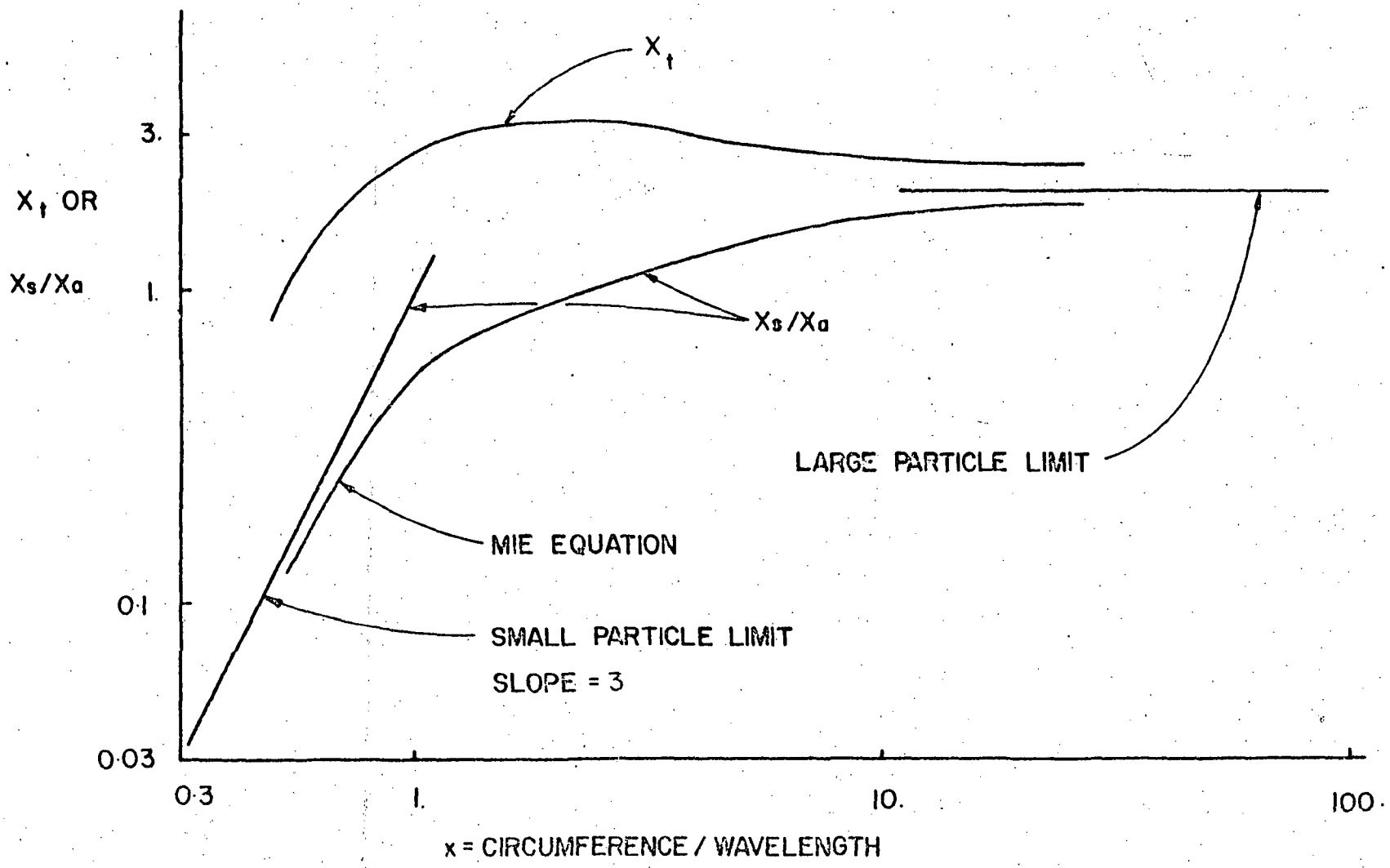
X_t
3.
X_t OR
X_s/X_a
1.
X_s/X_a
LARGE PARTICLE LIMIT
MIE EQUATION
0·1
SMALL PARTICLE LIMIT
SLOPE = 3
0·03
0·3
1.
10.
100.
x = CIRCUMFERENCE / WAVELENGTH

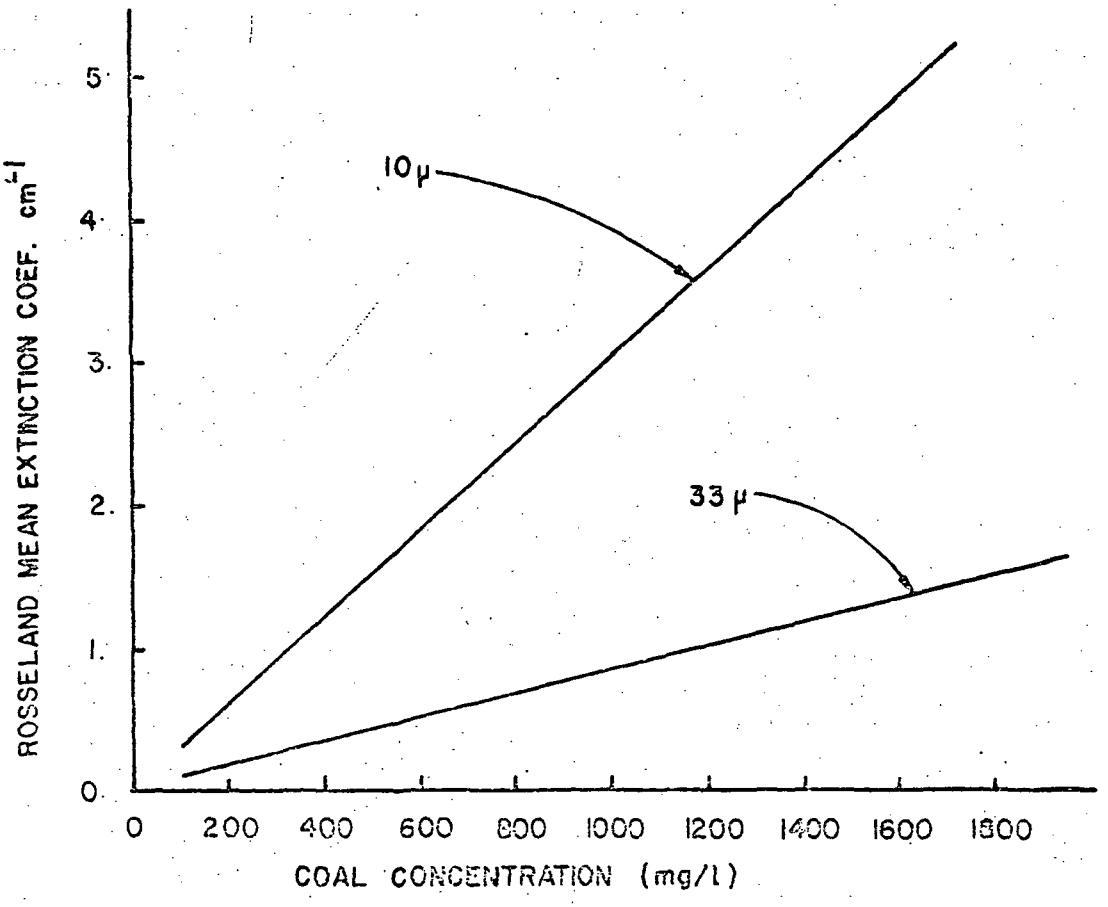
ROSSELAND MEAN EXTINCTION COEF. cm⁻¹
0
1.
2.
3.
4.
5.
10 μ
33 μ
0
200
400
600
800
1000
1200
1400
1600
1800
COAL CONCENTRATION (mg/l)

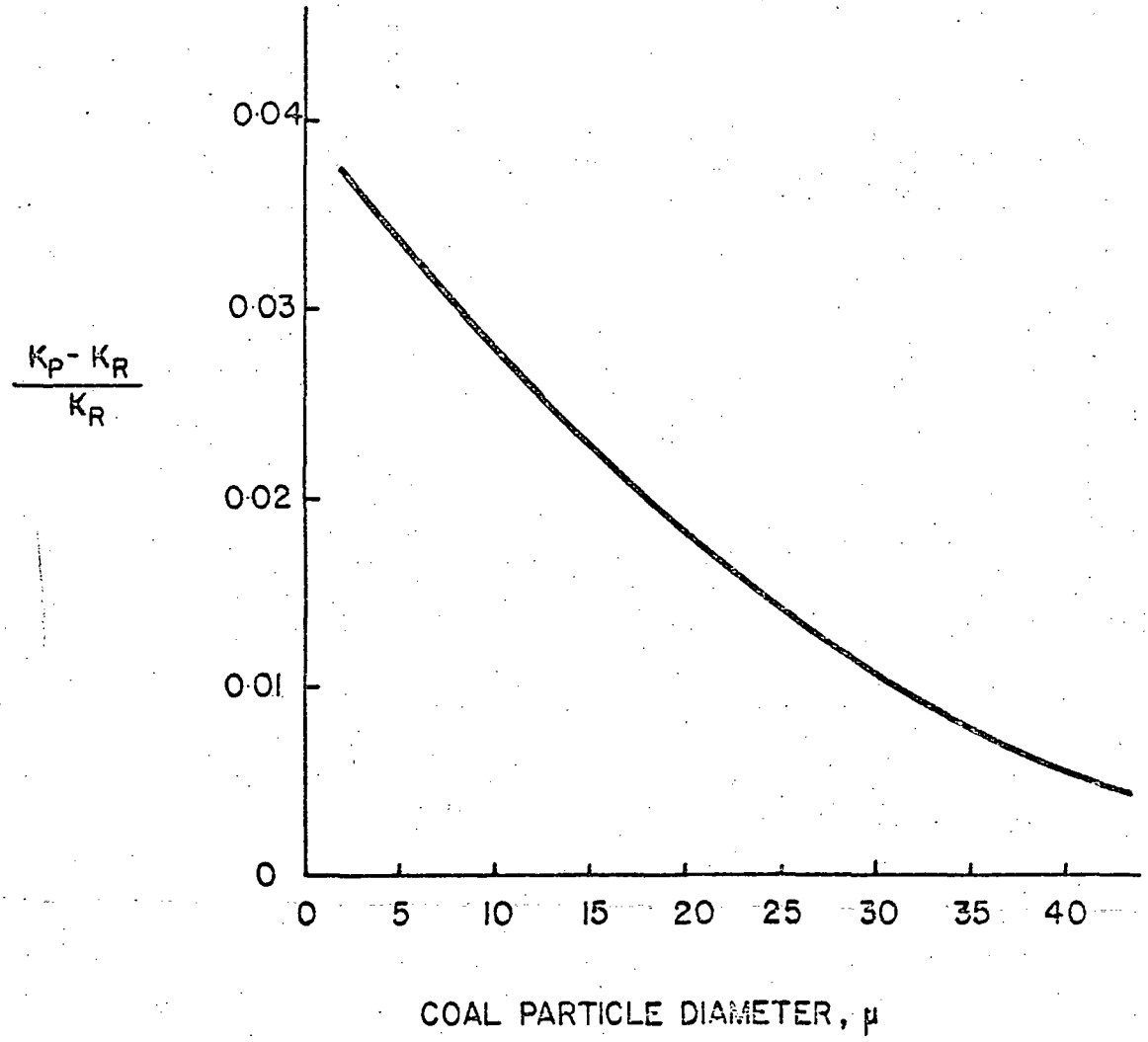
$\frac{K_P - K_R}{K_R}$
0·04
0·03
0·02
0·01
0
0
5
10
15
20
25
30
35
40
COAL PARTICLE DIAMETER, μ

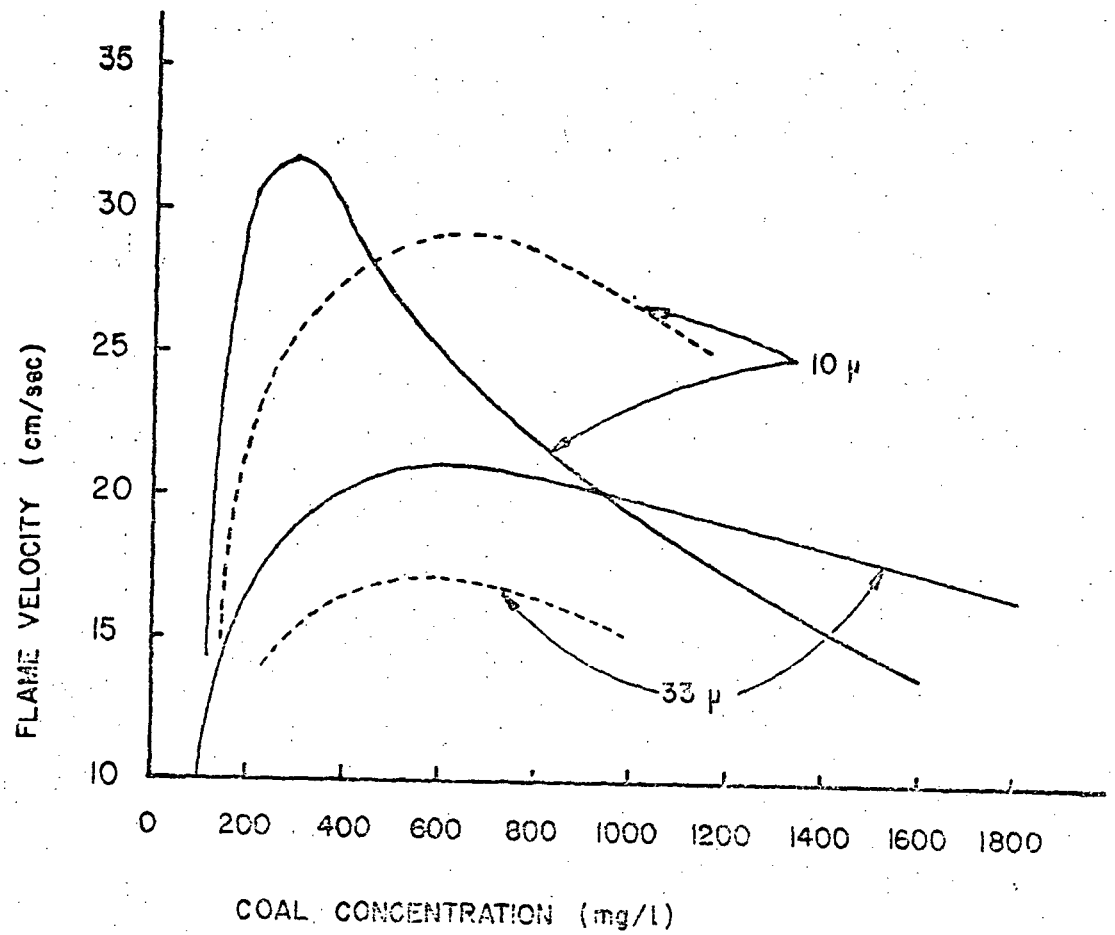
35
30
25
20
15
10
FLAME VELOCITY (cm/sec)
10 μ
33 μ
0
200
400
600
800
1000
1200
1400
1600
1800
COAL CONCENTRATION (mg/l)

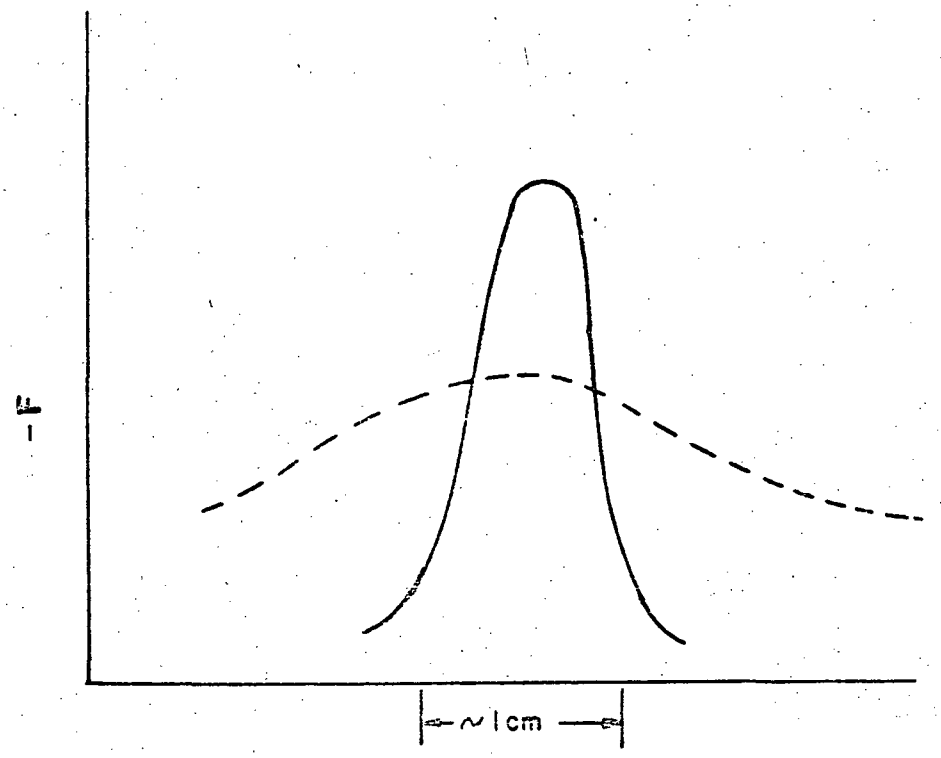
I
~1cm
DISTANCE

VIII. REFERENCES

1. Berlad, A. L.; Huggett, Clayton; Kaufman, Fred; Markstein, George; Palmer, H.B.; and Yang, C.H. "Study of Combustion Experiments in Space," NASA CR-134744 (November 1974).

2. Berlad, A.L. "Gravitational Effects on Combustion." INVITED PAPER. Progress in Astronautics and Aeronautics 52, 89-110 (1977) Ed. Leo Steg Publ. American Institute of Aeronautics on Astronautics.

3. Berlad, A.L. "Fluid and Combustion Dynamics." U.S. National Bureau of Standards Special Publication #570 (1978): "Applications of Space Flight in Materials Science and Technology."

4. Berlad, A.L. and Killory, J. "Flame Propagation and Extinction for Clouds of Particles." Paper presented at the March 28-30, 1977 Meeting of the Central States Section, The Combustion Institute.

5. Lavid, M. and Berlad, A.L. "Gravitational Effects on Chemically Reacting Laminar Boundary Layer Flows over a Horizontal Flat Plate." XVI Symposium (International) on Combustion, P. 1557 (1977). Pub: The Combustion Institute.

6. Smoot, L.D., Horton, M.D. and Williams, G.A. "Propagation of Laminar Pulverized Coal-Air Flames." XVI Symposium (International) on Combustion. P. 375 (1977).

7. McCaffrey, B.J. and Berlad, A.L. "Some Observations on the Oscillatory Behavior of Carbon Monoxide Oxidation." Combustion and Flame 26, 77 (1976).

8. Yang, C.H. and Berlad, A.L. "On the Kinetics and Kinetic Oscillation in Carbon Monoxide Oxidation." Transactions (I) of the Faraday Society, 70, 1661 (1974).

9. Berlad, A.L. and Krishna, C.R. "Gravitational Effects on the Autoignition of Particle Clouds." Paper presented at the Eastern States Section, The Combustion Institute (6-7 November, 1975).

10. Krishna, C.R. and Berlad, A.L. "Stability of Inhomogeneous Combustible Systems, Combustion and Flame 26, 133 (1976).

11. Berlad, A.L. "Thermokinetics and Combustion Phenomena in Nonflowing Gaseous Systems: An Invited Review." Combustion and Flame 21, 275-288 (1973).

12. Jacobsen, M., Cooper, A.R., and Nagy, J. "Explosibility of Metal Powders," Report RI6516 (1964).

13. Krishna, C.R. and Berlad, A.L. "A Model for Dust Cloud Autoignition." Combustion and Flame 37, 207 (1980).

14. Field, M.A., Gill, D.W., Morgan, B.B. and Hawksley, P.G.W. "Combustion of Pulverized Coal." The British Coal Utilization Research Association, 1967.

15. Merzanov, A.G., AIAAJ 13, 209 (1975).

16. Bandyopadhyay, S. and Bhaduri, D. Combustion and Flame 18, 411 (1972).

17. Cassel, H.M. and Liebman, I. Combustion and Flame 18, 467 (1959).

18. Andersen, H.C., and Belz, L.H. J. Electrochem. Soc. 100, 240 (1953).

19. Meese, R.A. and Skifstad, J.G., AIAAJ. 12, 71 (1974).

20. Rumanov, E.N. and Khaikin, B.I., Combustion, Explosion, Shockwaves 5, 129 (1969).

21. Berlad, A.L. and Yang, C.H. "A Theory of Flame Extinction Limits." Combustion and Flame 4, 325 (1960).

22. Berlad, A.L. "Inflammability Limits and Flame Radiation Loss Rates." Combustion and Flame 5, 389 (1961).

23. Williams, F.A. "Combustion Theory". Publ. Addison-Wesley (1965).

24. Berlad, A.L. and Killory, J. "Combustion of Porous Solids at Reduced Gravitational Conditions." NASA Contractor Report 3197 (Oct. 1979). Lewis Research Center of NASA.

25. Essenhigh, R.H. and Csaba, J. Ninth Symposium (International) on Combustion, p. 111. Pub.: The Combustion Institute (1963).

26. Nusselt, W. Z. Ver Dentoch. Ing. 68, 124 (1924).

27. Hottel, H.C., Sarofin, A.F. and Fabimian, E.J. Solar Energy 11, p. 3 (1967).

28. Wang, L.S. The Astrophysical Journal, 174, p. 671 (1972).

29. Eckert, E.R.G. and Drake, R.M. Jr. Analysis of Heat and Mass Transfer. p. 692. Pub.: McGraw-Hill (1972).

30. Dove, J.E. Dissertation (Oxford University) 1959.

31. Linnett, J.W., Reuben, B.G., and Wheatley, T.F. Combustion and Flame 12, 325 (1968).

32. Dickens, P.G., Dove, J.E., Linnett, J.W. Trans. Faraday Soc. 60, 539 (1964).

33. Minkoff, G.J. and Tipper, C.F.H. "Chemistry of Combustion Reactions." Pub.: Butterworths, London (1962).

34. McCaffrey, G.J. and Berlad, A.L. "Some Observations on the Behavior of Carbon Monoxide Oxidation". Combustion and Flame 26, 77 (1976).

35. Yang, C.H. and Berlad, A.L. "Kinetics and Kinetic Oscillation in Carbon Monoxide Oxidation." J. Chem. Soc., Faraday Transactions I, 70, 1661 (1974).

36. Gray, P., Griffiths, J.F., and Bond, J.R. "Carbon Monoxide Oxidation: Chemiluminescence and Ignition." XVII Symposium (International) on Combustion. Pub.: The Combustion Institute (Pittsburgh, Pa.) p. 811, 1978.

37. Yang, C.H. "On the Explosion, Glow, and Oscillation Phenomena in the Oxidation of Carbon Monoxide." Combustion and Flame 23, 97 (1974).

38. Gray, P., Jones, D.T., and MacKiven, R. "Thermal Effects Accompanying Spontaneous Ignition in Gases." Proc. Roy. Soc. (London) A325, 175 (Nov. 1971).